# BOND GRAPH MODELING OF A HYDRAULIC VIBRATION SYSTEM: SIMULATION AND CONTROL

**Farid Arvani, Geoff Rideout, Nick Krouglicof, Steve Butt**

Faculty of Engineering, Memorial University of Newfoundland, St. John's, Canada

(farvani, g.rideout, nickk, sdbutt) @mun.ca

## ABSTRACT

Electro hydraulic drives are often used where the dynamic response requirements of the driven load in terms of speed, cycling, accuracy and stability are particularly severe. One such application is the control and drive system associated with a high frequency hydraulic vibrator. A hydraulic shaker controls a valve which directs high pressure hydraulic fluid to generate controlled vibration. Hydraulic shakers typically have long stroke and large force and are useful up to many hundreds of Hertz vibration frequency.

In this paper, bond graph modeling is used to study and simulate the effect of various components in a hydraulic circuit on a shaker performance. The intention is that the electrohydraulic system vibrates at a specified force or displacement amplitude and frequency for the controlled vibration of a load attached to the rod. This paper describes the simulation and control of such system. Feedforward PID control scheme is utilized in the simulations to control the system and to track a variable reference signal.

Keywords: Hydraulics Actuator, Vibrator, Control System, Bond graph modeling

## 1. INTRODUCTION

Hydraulic control systems are used to control the position, speed or force of resisting loads. A linear hydraulic cylinder or a rotary-motion hydraulic motor usually provides the final drive. A positive displacement pump at a relatively high pressure between 7 and 35 MPa delivers the hydraulic fluid to the system to power the actuators.

Hydraulic control systems are used where relatively large forces and torques accompanied with fast, stiff response of resisting loads are required such as in industrial presses, machine tools and flight simulators, to name a few. They are used for closed-loop control of a response variable(s) such as in aircraft and industrial robot control; and in manual control over a substantial powered motion such as mobile equipment and road vehicle steering (Merritt 1967).

Understanding the hydraulic system dynamics plays an important role in designing controllers for ensuring a good system response or in finding out why an existing system is not performing satisfactorily (Dransfield 1981).

A typical hydraulic control system consists of a power supply, a flow control valve, an actuator, a transducer and a servo controller for closed-loop control. The control valve adjusts the flow of hydraulic fluid into actuator chambers to move the actuator to the desired position based on the control signal generated by the servo controller. A force control scheme operates similarly by using proper load transducer(s).

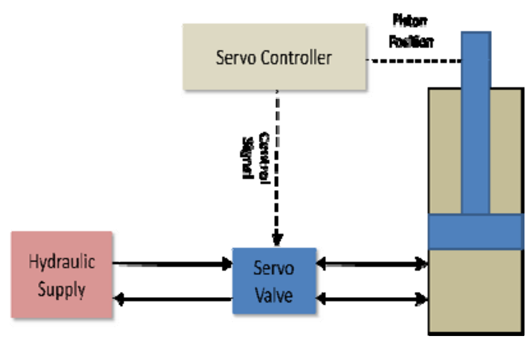


Figure 1: Schematics of the modeled hydraulic system

In this paper, the hydraulic dynamics of a valve-controlled hydraulic cylinder is developed and simulated, and a simplified model of a high frequency hydraulic system is presented. The models are derived from first principles and implemented using bond graph methodologies. Finally, a control system is proposed to perform a tracking control scheme for a hydraulic shaker. Figure 1 depicts the schematics of the modeled system. Solid lines show the bidirectional hydraulic signals while dashed lines designate the electrical control signals. Servovalves and actuators are the most important parts of this hydraulic system and therefore has been the main focus of this work. However other components have been modeled in detail as well.

## 2. MODELING METHODOLOGY

The simulated hydraulic circuit consists of the bond graph model of a closed–center four-way directional valve, hydraulic actuator, two pressure relief valves, three accumulators and four hydraulic hoses. 20-sim package is used to create and simulate the bond graphs. A tracking PID controller is implemented to perform position control on a linear actuator.

### 2.1. Servovalve modeling

This section describes the methodologies to model a servovalve which is generally comprised of a torque motor and a valve spool assembly (Jelali and Kroll 2003; Dransfield 1981; Poley 2005). The servovalve consists of a torque motor; application of electrical signal to its coil will generate a torque. The flapper of the torque meter is integrated with the spool assembly. The flapper acts as a mechanical feedback for the control of spool position (Maskrey 1978; Jones 1997; DeRose 2003).

The servovalves can be modeled using two approaches. The first method is to model the subcomponents of the valve. This requires the design parameters for the mechanical and electrical components of the valve. It is possible to derive meaningful transfer functions for electrohydraulic servovalves, and several papers have reported such work (Jelali and Kroll 2003). Unfortunately, servovalves are complex devices and have many nonlinear characteristics which are significant in their operation. These nonlinearities include: electrical hysteresis of the torque motor, change in torque-motor output with displacement, change in orifice fluid impedance with flow and with fluid characteristics, change in orifice discharge coefficient with pressure ratio, sliding friction of the spool, and others (DeRose 2003, Maskrey 1978).

Experience has shown that these nonlinear and non-ideal characteristics limit the usefulness of theoretical analysis of servovalve dynamics in systems design. Instead, the more meaningful approach is to approximate measured servovalve response with suitable transfer functions (Thayer 1965, Clarke 1969). Moog has performed sophisticated analyses of servovalve dynamic response including computer simulations of various nonlinear effects, and up to eight-order dynamics (excluding any load dynamics). The results indicate that these complex analyses have not contributed significantly to servovalve design due to uncertainties and inaccuracies associated with the higher-order effects.

#### 2.1.1. Servovalve Hydraulic Modeling

The actual flow through the valve is dependent upon electrical command signal and valve pressure drop. The flow for a given valve pressure drop can be calculated using the square root function for sharp edge orifices:

$$\mathrm{Q} = \mathrm{Q_N}\sqrt{\frac{\Delta \mathrm{P}}{\Delta \mathrm{P_N}}} \tag{1}$$

where Q [gpm] = calculated flow, $Q_N$ [gpm] = rated flow, $\Delta P$ [psi] = actual valve pressure drop and $\Delta P_N$ [psi] = rated valve pressure drop. The servovalve used in these simulations is high performance Moog- D765 series valves and the values for $Q_N$ and $\Delta P_N$ are provided in the valve datasheet. The modeled valve's schematics (Johnson 2008) is shown in figure 2.

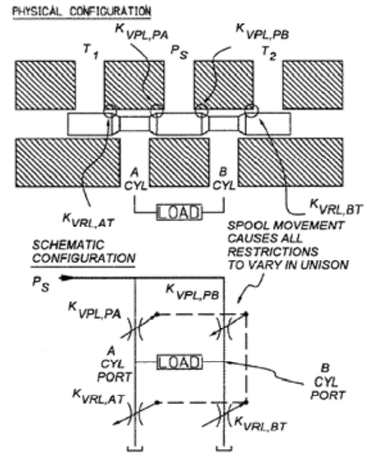


Figure 2: Physical and schematic configuration of the modeled valve (Johnson 2008)

The total valve coefficient is defined to be the flow coefficient at the flow rating conditions:

$$K_V = \frac{\mathrm{Q_N}}{\sqrt{\Delta \mathrm{P_N}}} \tag{2}$$

It is necessary to know the coefficient of each of the four lands. The valve ratio is defined as

$$\rho_V = \frac{K_{VPL}}{K_{VRL}} \tag{3}$$

where $K_{VPL}$ and $K_{VRL}$ have units of Holes and represent the valve coefficients for the pressure and return lines, respectively. It is safe to assume that valve ratio is unity in absence of evidence to the contrary as there is no reason to deliberately design a non-symmetrical valve. The relation between total valve coefficient and coefficients for valve lands is

$$K_{VPL} = K_V\sqrt{1+{\rho_V}^2} \tag{4}$$

$$K_{VRL} = K_V\frac{\sqrt{1+{\rho_V}^2}}{\rho_V} \tag{5}$$

The above equations are derived based on the fact that two orifice resistances are in series and are related by

$$K_V = \frac{K_{VPL}\,K_{VRL}}{\sqrt{{K_{VPL}}^2+{K_{VRL}}^2}} \tag{6}$$

It is noteworthy that these parameters take into account the spool geometry, discharge coefficient and oil density (Johnson 2008).

Servovalve delivers a control flow proportional to the spool position which is also proportional to the square root of the pressure drop across the valve. Combining equations (1) and (2) and comparing with the well known formula for flow–pressure relation for turbulent flow,

$$Q = C_d A \sqrt{\frac{2}{\rho}} \sqrt{\Delta P} \quad (7)$$

it is clear that $K_V$ provides us with the coefficient in the above formula easily which contains parameters for the spool geometry, discharge coefficient and oil density.

Torque motor can be modeled as a series L-R circuit, neglecting any back-EMF effects generated by the load (Poley 2005). The transfer function is

$$\frac{I(s)}{V(s)} = \frac{1}{sL_c + R_c} \quad (8)$$

where $R_c$ is the combined resistance of the motor coil and the current sensor resistor of the servo amplifier and $L_c$ is the inductance of the motor coil. Values of these parameters for series and parallel wiring configurations of the motor are published in the manufacturer's data sheet.

Control flow, input current and valve pressure drop are related by

$$Q = K_V \times i_V \times \sqrt{\Delta P} \quad (9)$$

where $i_V$ is the input command corresponding to a specific valve opening and $\Delta P$, pressure drop across the valve, is given by $\Delta P = P_s - P_T - P_L$ where $P_s$, $P_T$ and $P_L$ are system pressure, return line pressure and load pressure, respectively. The change in flowrate with current and load pressure is shown in figure 3.

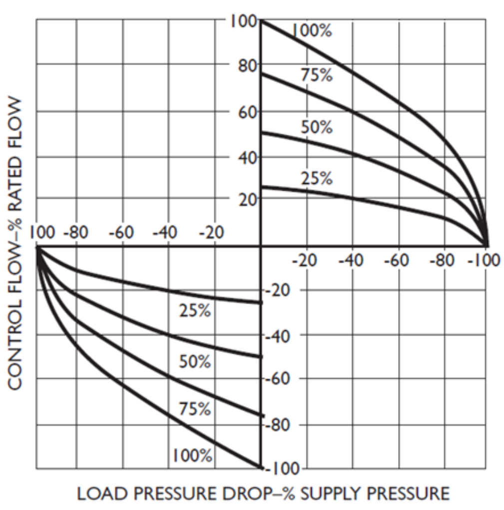


Figure 3: Relationship between flowrate and pressure drop across a servovalve for different input command percentages (Johnson 2008)

The servovalve is not the primary dynamic element in a typical hydraulic servo valve. The servo valves are sized in a way that its natural frequency is at least three times the natural frequency of the hydraulic actuator and therefore it is only necessary to model the valve for a low range of frequencies without major accuracy loss.

A typical performance graph for a high-response servo-valve Moog D765 is shown in figure 4 where the frequency response of the valve is plotted for different command percentages, taken from the manufacturer's datasheet.

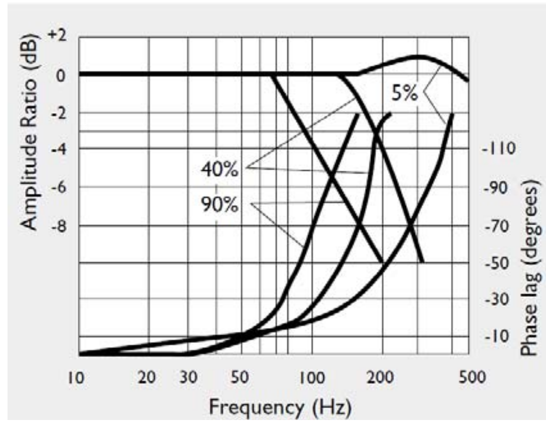


Figure 4: Frequency response of Moog D765 servovalve (Courtesy of Moog Inc.)

A second order model yields an approximation to actual behavior. Standard second order system identification of the frequency response can be performed where suitable values for natural frequency and damping ratio will need to be determined from the graph. Natural frequency ($\omega_V$) can be read fairly accurately from the -3dB or 90 degree phase point of the 5% curve in figure 4. Damping can be determined from an estimate of the magnitude of the peaking present. For an under-damped second order system, the damping factor ($S_V$) can be shown to be related to peak amplitude ratio ($M_V$) by the formula (Poley 2005).

$$M_V = \frac{1}{2\zeta_V \sqrt{1 - \zeta_V^2}} \quad (10)$$

A reasonable estimate of peaking based on the 5% response curve would be about 1.5 dB, which corresponds to an amplitude ratio of about 1.189. Solving the above equation, a value of damping is determined to be about $\zeta_V = 0.48$. Using these values, a model of the servo-valve spool dynamics may be constructed. The input to the model will be the torque motor current normalized to the saturation current obtained from the datasheet, and the output will be the normalized spool position. SIMULNK modeling is used to obtain the simulated frequency response of the transfer function for 5% opening (shown in figure 5).

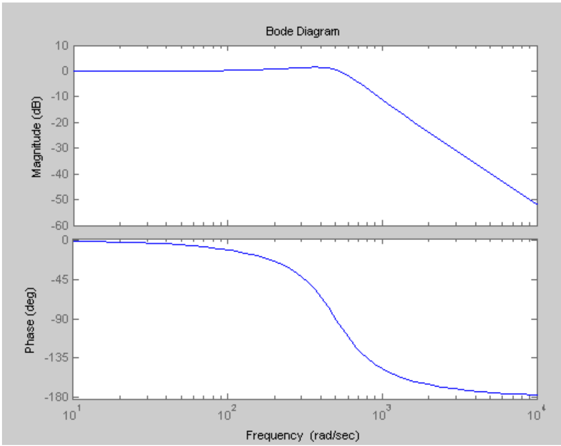


Figure 5: Simulated frequency response of Moog D765 valve

The step response of the servo valve is shown in figure 6. The open loop settling time is 0.04s.

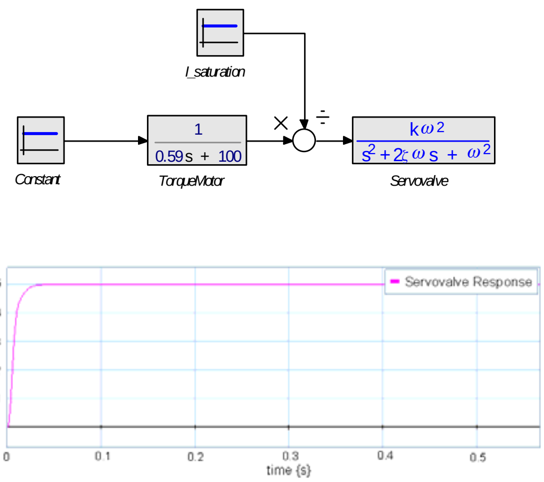


Figure 6: Transfer function for valve spool positioning system and its step response

### 2.1.2. Servovalve Bond Graph Modeling

The nonlinear pressure-flow relation is modeled using the *modulated R-elements* for each valve land utilizing the equations and formulation in section 2.1.1.

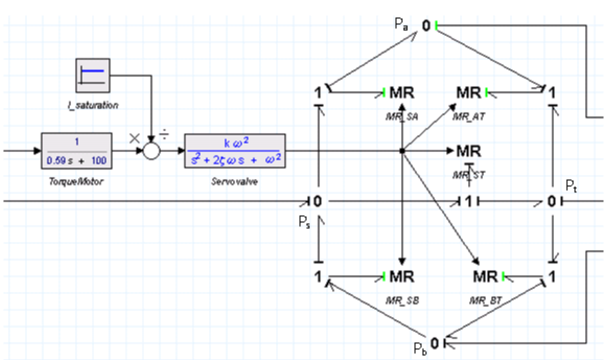


Figure 7: Bond graph model of the servo valve

The model of the torque motor and the servovalve dynamics is described in the previous section. The values for the parameters are taken from the manufacturer's data sheet. *Modulated resistors* are used to model the sharp edge orifices. As it is shown in figure 7, the modulated resistors are located between pressure drops between four valve ports. $P_s$, $P_a$, $P_b$ and $P_t$ represent supply pressure, port A and B pressures and return line pressure, respectively. The spool position is provided by the valve dynamics computed by the transfer functions and the *R-elements* are modulated by the value of the spool position. In this model, the pressures of port A and B of the valve are respectively connected to the actuator chambers A and B. Port S is connected to an effort source which models an ideal source of power capable of supplying constant pressure at any flow required (Muvengei and Kihiu 2010). Port T is the pressure for the return line. The infinitesimal leakage between port S and T is also modeled as a *Resistor*.

### 2.2. Actuator Modeling

The model of the actuator consists of two *C-elements* for each chamber. These capacitors model the oil compressibility in the chambers. It is notable that while the piston rod is retracting or extending, the chamber volume is changing and therefore two modulated capacitors are used to model this effect. The leakage is modeled using Hagen-Poisseille equation (Muvengei and Kihiu 2010). The position of the piston is controlled by the modulation of the *I–element*. The model is shown in figure 8.

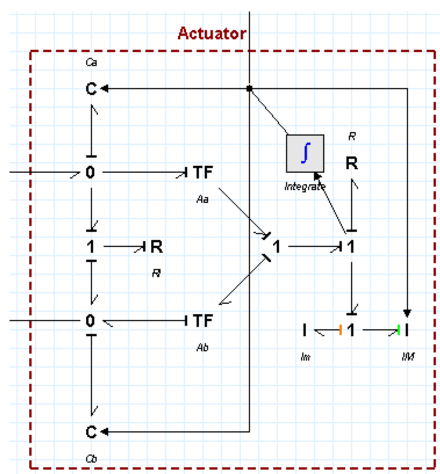


Figure 8: Bond graph model of the linear actuator

### 2.3. Pressure Relief Valve Model

The pressure relief valve is modeled (shown in figure 9) so that if the pressure is above a threshold, it will bleed the hydraulic fluid to generate balanced pressure.

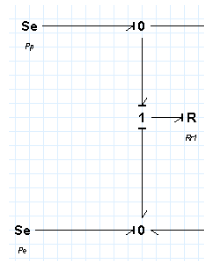


Figure 9: Bond graph model of the pressure relief valve

### 2.4. Hoses Model

There are four hoses that run between the servovalve, pump and the actuator. Compliance elements are included to take the expansion of the tubes radially, and oil compressibility into account. An *R-element* for the pressure loss due to the wall friction in the hose is also considered (Hölcke 2002). An *I-element* is added to account for the fluid inertia (Karnopp, Margolis, and Rosenberg 2006).

### 2.5. Bond Graph Model of Hydraulic Circuit

The full bond graph model using the subcomponents of the previous subsections is shown in figure 10. This model includes the model of the servovalve, two pressure relief valves, three accumulators and four corresponding hydraulic hoses. This model is simplified by removing the models for the accumulators and the hoses for simplification in analysis and using a PID controller to perform position control.

## 3. CONTROLLER DESIGN AND SIMULATION

In this section, a feedforward PID is implemented to simulate the desired motion on the actuator (Caputo 1996). The controller utilizes the piston position of the actuator as a feedback signal which is obtained by the integration at the *I-element* associated with the piston. The generated model is used to perform PID control on two scenarios. The following figure shows the complete bond graph model with the implemented control.

First a constant reference position is used to carry out position control on the cylinder. The stroke length is 30cm and the initial position of the piston is 15cm. The controller will extend the piston 5 cm and stop (shown in figure 11).

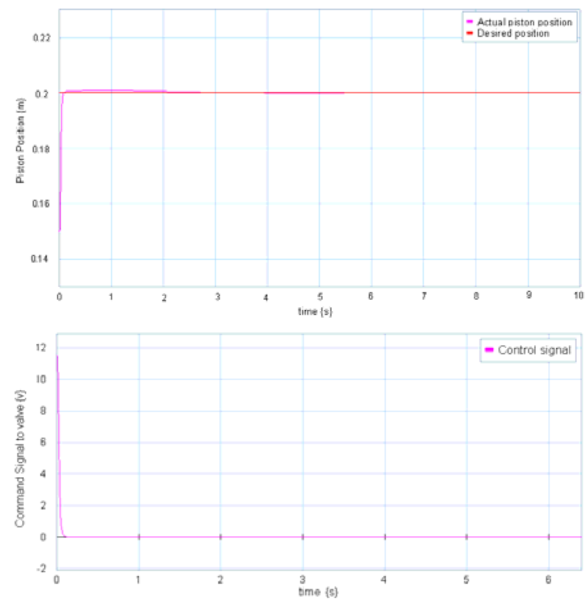


Figure 11: Step response of the system for 5cm movement – Desired and actual piston location (above) and corresponding control signal (below)

In the second scenario, a sinusoidal profile is used to perform target tracking to simulate the behavior of the system for oscillation generation. In this case, a sinusoidal signal, is used to perform position tracking and as it is shown in the figure 12, it can perform the tracking with a good performance. The control signal to the valve is shown in figure 12.

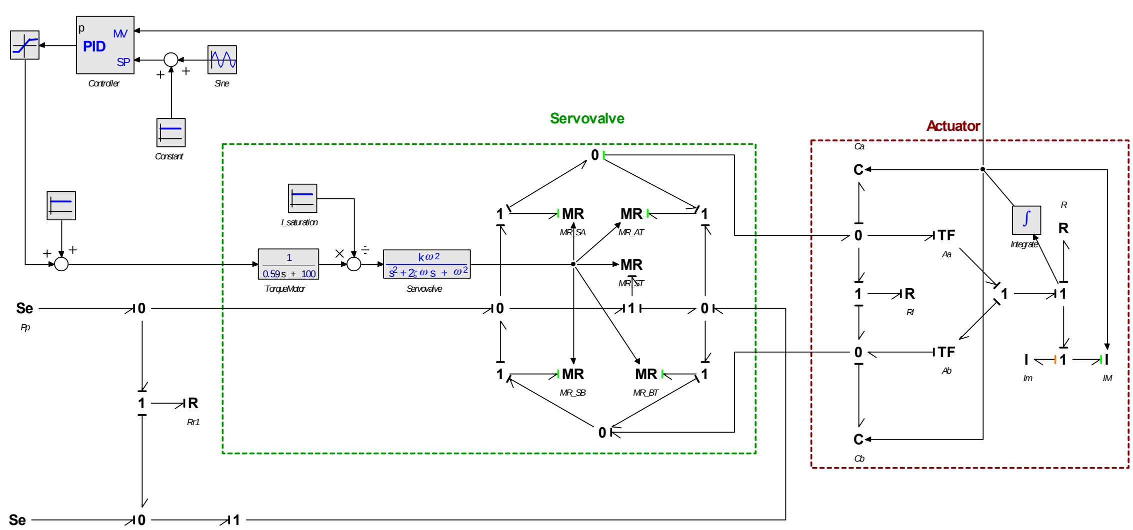


Figure 10: Bond graph model of the hydraulic system

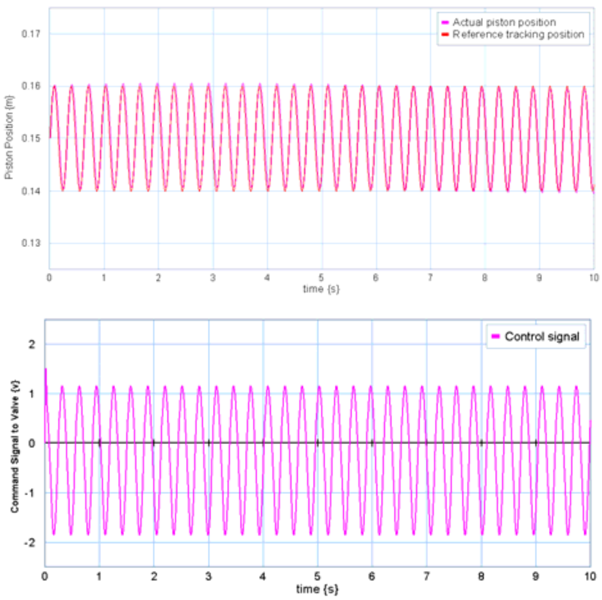


Figure 12: Response of the system for sinusoidal piston movement – Desired and actual piston location (above) and corresponding control signal (below)

Feedforward PID controller enables increased dynamic system responsiveness while decreasing positioning and velocity error. Feedforward gains are predictive gains that contribute to the control signal in the form of a linear combination of the target velocity and acceleration terms. The result is higher performance and durable machine control due to smoother motion. The control signal is applied to the valve and in both cases is appropriate in the sense that they do not excite the valve with jerk that usually causes immature failure of the components.

## APPENDIX A - PARAMETERS AND SYMBOLS

| Symbol | Description | Value |
|---|---|---|
| $\rho$ | Oil Density | 867 kg/$m^3$ |
| $A_{h1}$ | Hose 1 Area | 0.000791 $m^2$ ( 1 ¼”) |
| $A_{h2}$ | Hose 2 Area | 0.000506 $m^2$ ( 1”) |
| $L_{h1}$ | Hose 1 length | 20 cm |
| $L_{h2}$ | Hose 2 length | 20 cm |
| $\upsilon$ | Kinematic Fluid Viscosity | 27cSt |
| $\mu$ | Absolute Fluid Viscosity | 0.023409 Pa.s |
| B | Bulk modulus of Oil | 1.5 GPa |
| E | Elastic Modulus of hydraulic hoses | 30 MPa |
| m | Rod and piston mass | 2.5 kg |
| M | Load mass | 500kg |

| Actuator parameters | |
|---|---|
| **Description** | **Value** |
| Rod Diameter | 1 ¾” |
| Piston Diameter | 2 ½” |
| Length of cylinder | 0.3m |
| Length of piston | 0.01m |

## REFERENCES


Merritt, H. E., 1967. *Hydraulic Control Systems*. New York: John Wiley and Sons.

Jelali, M. and Kroll, A., 2003. *Hydraulic Servo Systems- Modelling, Identification and Control*, Springer Verlag.

Dransfield, P., 1981. *Hydraulic Control systems- Design and Analysis of Their Dynamics*. Springer Verlag.

Muvengei, M. and Kihiu, J., 2010. Bond Graph Modeling of Inter-Actuator Interactions in a Multi-Cylinder Hydraulic System. *International Journal of Mechanical, Industrial and Aerospace Engineering*. *World Academy of Science, Engineering and Technology*, 32-41.

Johnson, J.L, 2008. *Designer`s Handbook for Electrohydraulic Servo and Proportional Systems*. 4th edition. IDAS Engineering Inc.

Karnopp, D. C., Margolis, D. L, and Rosenberg, R. C., 2006. *System Dynamics: Modelling and Simulation of Mechatronic Systems*. 4th edition. New York:John Wiley and Sons.

Maskrey, R.H. and Thayer, W.J., 1978. A Brief History of Electrohydraulic Servomechanisms. *ASME Journal of Dynamic Systems, Measurement and Control* Vol 100, No 2, pp 110-116.

Thayer, W.J., 1965. Transfer Functions for Moog Servovalves. *Technical Bulletin 103*. Moog Inc.

Jones, J.C., 1997. Developments in Design of Electrohydraulic Control Valves. *Technical Paper*. Moog Inc.

Clarke, D.C., 1969. Selection and Performance Criteria for Electrohydraulic Servovalves. *Technical Bulletin 103*. Moog Inc.

DeRose, D., 2003. Proportional and Servo Valve Technology. *Fluid Power Journal*. March/April, 8-15.

Caputo, D., 1996. Digital Motion Control for Position and Force Loops. Proc. National Conference Confreence. Fluid Power. Vol: Issue 47th:263 Vol 1-268.

Hölcke, J., 2002. *Frequency Response of Hydraulic Hoses*. Licentiate Thesis. Royal Institute of Technology, KTH, Stockholm.

Poley, R., 2005. DSP Control of Electro-Hydraulic Servo Actuators. *Application Report* SPRAA76. Texas: Texas Instruments.

D765 Series Servovalves. *Product Datasheet*. Moog Inc.

20sim version 4.1. Controllab Products B.V.. Enchede, Netherlands. http://www.rt.el.utwente.nl/20sim/.